Competition between mixing and segregation in bimetallic Ag_nRb_n clusters (n = 2–10)[1,2]

René Fournier, Shaima Zamiruddin, and Min Zhang

Abstract: We found the minimum-energy structures of Ag_nRb_n (n = 2–10) clusters by a combination of density functional theory (DFT) and taboo search global optimization. The global minimum geometry is mixed for $n \leq 4$ and segregated, with a core-shell arrangement, for $n > 4$. There is a change in the nature of the bonding, from ionic to metallic, between $n = 4$ and $n = 5$. Although metallic bonding dominates at $n > 4$, large atomic charges (in the order of ±0.5) persist. These atomic charges (negative on the interior Ag atoms, positive on the surface Rb atoms) make Ag_nRb_n clusters analogous to Zintl compounds and could prevent them from coalescing. This makes them intriguing potential building blocks for cluster-assembled materials. Ag_4Rb_4 is relatively stable compared with other Ag_nRb_n clusters; it has a nearly cubic shape, a large HOMO–LUMO gap (2 eV), and a highly ionic character with atomic charges equal to roughly ±1 au.

Key words: bimetallic clusters, nanostructured materials, global energy minima, segregation, Zintl compounds.

Résumé : Nous avons déterminé les structures d'énergie minimum d'agrégats Ag_nRb_n (n = 2–10) par une méthode qui combine la théorie de la fonctionelle de la densité avec une recherche de minima par optimisation globale (recherche tabou). Les minima globaux que nous obtenons sont des structures mixtes d'alliages pour $n \leq 4$, et des structures ségrégationnée de topologie concentrique $Ag_n@Rb_n$, pour $n > 4$. La nature des liens évolue en fonction de n, avec de fortes interactions ioniques pour $n \leq 4$ et des liens de type métallique pour $n > 4$. Cependant, des charge atomiques appréciables subsistent à $n > 4$ (charges négatives sur les atomes de Ag qui sont à l'intérieur, et charges positives sur les atomes de Rb en surface). La séparation radiale des charges rend les agrégats de Ag_nRb_n analogues aux composés Zintl, et les rend probablement stables vis-à-vis la coalescence. Cette propriété ferait des agrégats de Ag_nRb_n des unités de base intéressantes pour d'éventuels matériaux. Ag_4Rb_4 est relativement stable comparé aux autres agrégats de Ag_nRb_n et possède une structure cubique ainsi qu'une forte séparation des niveaux d'énergie des orbitales frontières (2 eV) et un fort caractère ionique avec des charges atomiques de l'ordre de ±1 au.

Mots-clés : agrégats bimétalliques, matériaux à l'échelle du nanomètre, minima globaux d'énergie, ségrégation, composés Zintl.

Introduction

The structure of small metal clusters, and particularly "bimetallic" clusters, are not well-known. The phase diagrams of bulk alloys do not give reliable predictions about possible mixing in the corresponding small bimetallic clusters.[3] For alloying, as for many other things, clusters are often very different from the bulk. Many simple questions about bimetallics A_nB_p are still open. Generally, one would like to know if A and B segregate, or if they mix to form a nanoalloy. Experimentally, the structures of bimetallic clusters A_nB_p often fall into one of these three categories: mixed, core-shell, or onion-layered.[4] There is also a fourth category, "left-right segregated", that often occurs in the bulk limit because it minimizes the A–B interfacial area. A recent computational study showed that Pd–Pt clusters described by a Gupta potential adopt different types of segregated structures depending on the value of A–B interaction parameters used in the potential.[5] One could also distinguish between various mixed structures, some of them ordered, others, random. In fact, the details of A–B ordering can be intricate even in simple theoretical models of coinage (Cu, Ag, Au) bimetallic clusters.[6]

We chose to study the series of clusters Ag_nRb_n (n = 2–10) as a model to test computational methods and tackle general questions about AB order in bimetallic clusters because (*a*) it is simple (Ag and Rb atoms have only s valence electrons), (*b*) the big difference in absolute electronegativity $\chi = (I + A)/2$ (I is the ionization energy, A is the electron affinity, χ = 4.44 eV for Ag, and χ = 2.33 eV for Rb) favors mixing but, (*c*) the big difference in cohesive energies (2.95 eV for Ag, 0.85 eV for Rb) and atomic radii (1.45 Å for Ag, 2.42 Å for Rb) favor core-shell segregation. We expect (*c*) to dominate and control the structure at large n. But small clusters, where there are few or no interior atoms, could be very different, and the size evolution of structure is non-trivial. The nature of the bonding in these small clusters is also unclear a priori. Ag and Rb both have a very low ionization energy, and many aspects of Ag_n[7] and Rb_n[8] clusters are reasonably

Received 18 December 2008. Accepted 19 March 2009. Published on the NRC Research Press Web site at canjchem.nrc.ca on 23 June 2009.

R. Fournier[1] and S. Zamiruddin. Department of Chemistry, York University, Toronto, ON M3J 1P3, Canada.
M. Zhang. Department of Physics, York University, Toronto, ON M3J 1P3, Canada.

[1]Corresponding author (e-mail: renef@yorku.ca).

well-described in the jellium model.[9] So, in a way, Ag and Rb are ideal metals. But in Ag_nRb_n, ionic interactions could be important, and maybe small clusters of Ag_nRb_n are not even metallic, after all. Clusters like Ag_nRb_n are interesting for another reason. Their presumed core-shell structure, combined to large surface charges, should prevent them from coalescing. This is important for making cluster-assembed materials. For instance, size-selected metastable $Ag_n@Rb_n$ or $Ag_n@Na_n$ clusters (the @ symbol denotes a core-shell structure with the Ag atoms inside) could be relatively stable intermediates on the way to making uniform size silver clusters embedded in ionic solids (e.g., RbCl, NaCl). In fact, one can view $Ag_n@Rb_n$ as a metal cluster analog of Zintl compounds, with a true metal (Ag) in the interior instead of a semimetal (Ge, Sn, Pb, Sb, and so forth) like in the known Zintl compounds,[10] so there is a slight possibility that it could be stable in itself.

Methods

We performed global optimization by the taboo search in descriptor space (TSDS) method.[11] All energies were calculated by density functional theory (DFT) with the Perdew–Burke–Ernzerhof (PBE)[12] generalized gradient approximation to exchange-correlation and a LANL2 double-zeta (LANL2DZ) basis set as implemented in the Gaussian 03 software package.[13] The number of possibles isomers (local minima) for elemental clusters X_n is quite large; for a 13-atom cluster, it is in the order of 1000, and the number of isomers roughly triples for every additional atom.[14] However, the number of isomers for a bimetallic cluster A_nB_n is much greater than for an elemental cluster X_{2n}. Ignoring symmetry, there are $(2n)!/(n!)^2$ ways to substitute n atoms of X by atoms of A (and the rest by atoms of B). The $(2n)!/(n!)^2$ isomers of A_nB_n that result from these different ways to occupy sites with atoms of type A or B are often called "homotops".[15] For $Ag_{10}Rb_{10}$, then, an order of magnitude estimate for the number of isomers is 10^{11}. Fortunately, the optimization problem is not as difficult as it seems because the vast majority of isomers are very high in energy, *and the low-energy isomers fall into one or a few categories that share common geometric characteristics*. The TSDS algorithm exploits these resemblences among low-energy structures to quickly identify regions of configuration space where the search is likely to succeed, and it finds GMs, or good approximations to them, with very few energy evaluations even in difficult cases.[16,17] The TSDS runs for this study consisted of $(12n^2 + 30)$ iterations, where $2n$ is the number of atoms. At every iteration, TSDS produces a structure of Ag_nRb_n with predefined nearest-neighbour (NN) distances. A few preliminary runs of local optimization on arbitrary trial geometries of small Ag_nRb_n clusters show what distances are appropriate, and they were set at 2.82 Å for Ag–Ag, 4.70 Å for Rb–Rb, and 3.65 Å for Ag–Rb. For comparison, the bulk experimental interatomic distances are 2.89 Å for Ag–Ag and 4.84 Å for Rb–Rb. Other control parameters in TSDS ensure that the majority of the $(12n^2 + 30)$ structures generated in this way are topologically distinct, but a fraction of them are "distorted copies" of previous structures. These $(12n^2 + 30)$ geometries are not local minima of the potential surface, but are near local minima. For this reason, our optimization algorithm can be viewed as having an additional approximation compared to basin hopping (BH) methods,[18] but having the advantage of being much more economical (by roughly a factor of 50) compared to BH in terms of the number of energy evaluations required. The last point is, of course, crucial for doing global optimization directly on a first-principles DFT energy surface. After the TSDS iterations are complete, the $(12n^2 + 30)$ structures are ordered according to their energy and their similarity to higher ranked structures, i.e., similar structures get pushed down the ranks. The 10 to 20 top in this order constitute the lowest energy-distinct structures: we take them as initial geometries for local optimization with Gaussian 03 PBE/LANL2DZ.

To analyze trends in the final optimized structures, we use a number of geometric descriptors. Note that these are, generally speaking, different from the descriptors used during TSDS optimization. The three basic descriptors that we use for characterizing AB order are the number of A–B NN pairs m, and two variables, c and ℓ, that quantify core-shell segregation (CSS) and left–right segregation (LRS), respectively. In the following equations, a and b are indices that label atoms of type A and B, respectively, d_{ab} is the distance between a A–B pair of atoms, R_A and R_B are the atomic radii for elements A and B, $R_{AB} = R_A \pm R_B$, $\vec{P}_a$ and $\vec{P}_b$ are position vectors of the nuclei, and $\vec{C}$ is the center of mass of the cluster calculated with fictitious masses of one for all atoms. We use a simple cut-off function of interatomic distance $f(d_{ab})$ to decide if two atoms are neighbours, and add up to get the number of AB neighbour pairs.

$$\begin{aligned} f(d_{ab}) &= 1 \text{ if } d_{ab} < 1.1R_{AB} \\ &= [1.3R_{AB} - d_{ab}]/0.2R_{AB} \text{ if } 1.1 \le d_{ab}/R_{AB} \le 1.3 \\ &= 0 \text{ if } 1.3R_{AB} < d_{ab} \\ m &= 1/2\sum_{a=1}^{n}\sum_{b=1}^{n} f(d_{ab}) \end{aligned} \quad [1]$$

The two segregation variables are simple relations between centers of mass of different types of atoms.

$$\ell = \frac{1}{n}\left|\sum_{a=1}^{n}\vec{P}_a - \sum_{b=1}^{n}\vec{P}_b\right| \quad [2]$$

$$c = \frac{1}{n}\left[\sum_{a=1}^{n}|\vec{P}_a - \vec{C}| - \sum_{b=1}^{n}|\vec{P}_b - \vec{C}|\right] \quad [3]$$

We normally do not use m, ℓ, or c directly. Instead, we calculate m, ℓ, and c for all the homotops of a given structure, or a large sample of those homotops, and estimate the average "Avg" and standard deviation "SD" of m, ℓ, and c over the sample set of homotops. We sample homotops by doing a long sequence of random A–B position interchanges, calculating m, ℓ, and c each time. We denote the values of the variables for the structure itself (parent homotop) m_0, ℓ_0, and c_0, and define relative descriptors like this:

$$M = \frac{m_0 - \text{Avg}(m)}{\text{SD}(m)} \quad [4]$$

$$L = \frac{\ell_0 - \text{Avg}(\ell)}{\text{SD}(\ell)} \quad [5]$$

Fig. 1. Isomers of Ag_3Rb_3 and their relative energies (eV).

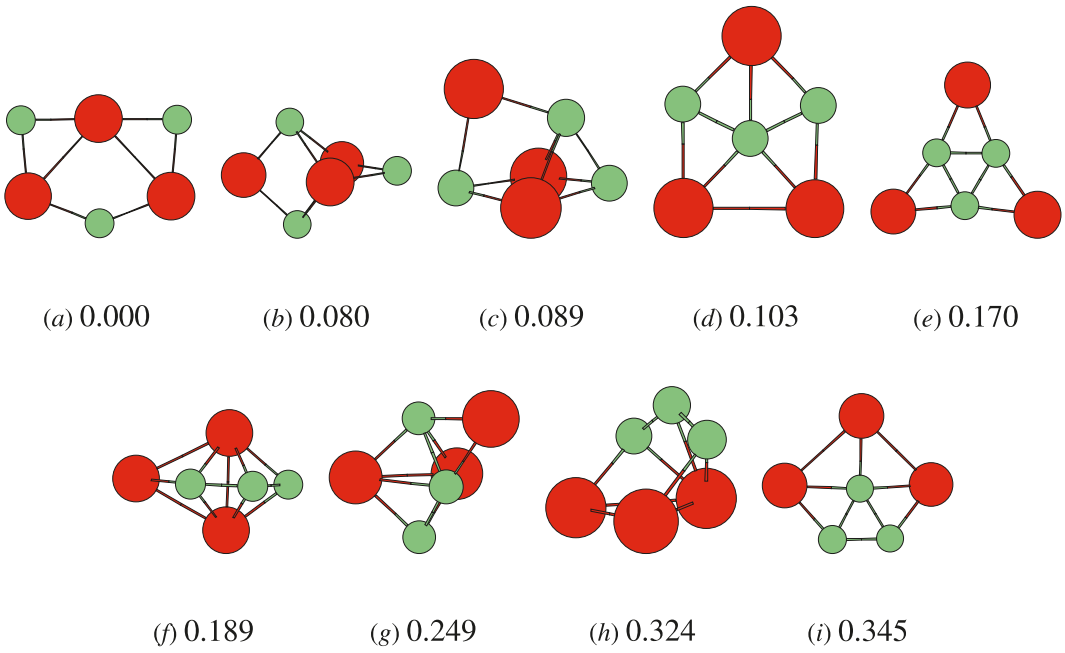

$$[6] \qquad C = \frac{c_0 - \mathrm{Avg}(c)}{\mathrm{SD}(c)}$$

So, for instance, an M value of +2.00 means that this structure has a number of A–B nearest neighbours that is larger than the average value for all of its homotops by two standard deviations; a value of zero for ℓ means that the structure has a degree of left–right segregation that is average relative to the set of all homotops to which it belongs, and so forth. Another variable that we use to quantify core-shell separation is the number of interior atoms N_i defined as follows: First, we calculate the asphericity ζ_j around each atom j by

$$[7] \qquad \zeta_j = \frac{(I_a - I_b)^2 + (I_b - I_c)^2 + (I_c - I_a)^2}{I_a^2 + I_b^2 + I_c^2}$$

where I_a, I_b, and I_c are the moments of inertia of the *neighbours* of atom j. We assign, to atom j, a number $n_j = \exp(-(\zeta_j/\zeta_0)^2)$, which tends to be close to one for interior atoms and close to zero for surface atoms, and get an effective number of interior atoms, N_i, by adding up the n_j's.

$$[8] \qquad N_i = \sum_j n_j = \sum_j \exp\left(-(\zeta_j/\zeta_0)^2\right)$$

With these definitions and $\zeta_0 = 0.0601$, we almost always get $n_j > 0.9$ for atoms that we would have classified as "interior atoms" upon visual inspection and $n_j < 10^{-5}$ for typical surface atoms. Another descriptor of geometry that we use is F_{90}, the number of 90° angles per atom. It is defined by

$$[9] \qquad F_{90} = \frac{1}{2n}\sum_j \sum_{k>\ell} \cos(\theta_{kjl} - 90^\circ)^{100}$$

where k and ℓ index the neighbours of atom j. The exponent 100 in that formula is arbitrary, but it produces an intuitively correct count of the number of right angles.

Results and discussion

A taboo search explicitly encourages diverse solutions; therefore, it not only has a good chance of finding the global minimum (GM), but it is also likely to find many of the lowest-energy isomers. This is illustrated in Fig. 1, which shows the nine isomers found for Ag_3Rb_3 (another structure found by TSDS turned out to be a repeat of the 0.080 eV isomer). We should say a few words to put our results in perspective. We estimate that DFT-PBE gives errors of roughly 0.1 eV to 0.2 eV on relative cluster isomer energies for elements with low cohesive energy like Ag and Rb, and we believe that it is unlikely that TSDS would miss the GM but it is more likely that it would miss some (and maybe many) of the low-energy isomers. That said, there is clearly a lot of diversity among the lowest-energy structures of Ag_3Rb_3 some flat and some tridimensional, some well-mixed (e.g., 0.000 eV) and some segregated (e.g., 0.324 eV). The same is true for Ag_5Rb_5 (four very different isomers found within 0.1 eV, see Fig. 2) and Ag_6Rb_6 (three very different isomers found within 0.1 eV). The Ag_9Rb_9 and $Ag_{10}Rb_{10}$ clusters also have many isomers within 0.1 eV of the GM, but those isomers are similar, all of them have a silver core and an incomplete rubidium shell. In Fig. 3, we show the distribution of isomer energies as a function of n, and the cohesive energies of GM as a function of $N^{-1/3}$ ($N = 2n$). The number of isomers within a small energy range of the GM varies a lot. We did not find any isomer within 0.2 eV of the GM at n = 2, 4, and 8 but found five for n = 3, six for n = 5, four for n = 6, one for n = 7, four for n = 9, and six for n = 10 (some of them are indistinguishable in Fig. 3*a*).

Notwithstanding the uncertainty about the identity of the GM, it is convenient to focus on the structures and properties of the putative GM to see how they evolve with size (Figs. 3 and 4). Cohesive energies $E(N)$ of the GM (Fig. 3*b*) follow a typical trend for metal clusters; they are well-fitted by the function $E(N) = E_{bulk} + bN^{-1/3}$, with a

Fig. 2. Isomers of Ag_nRb_n ($n > 3$) within 0.10 eV of the GM and their relative energies.

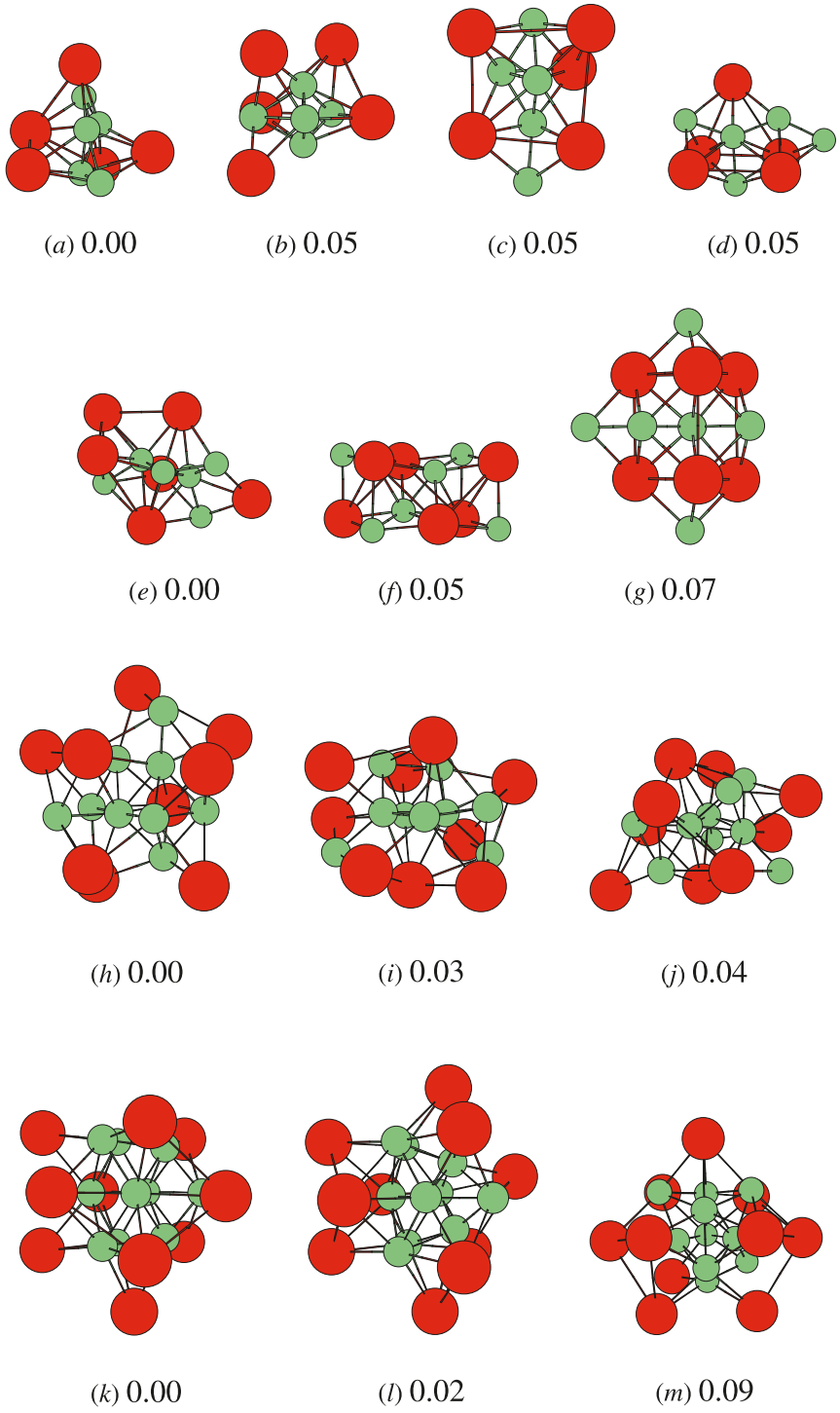

correlation coefficient of –0.9918. The intercept E_{bulk} is 1.75 eV/atom, which is 8% smaller than the average of experimental cohesive energies for Ag (2.95) and Rb (0.85). The negative of the slope (1.26) is related to surface energy: it is much smaller than the negative of the slope (3.48) that we got by fitting the Ag_n cohesive energies obtained years ago in another series of DFT calculations.[7] This is not surprising considering that the surfaces of Ag_nRb_n clusters are enriched in Rb atoms. Generally, for elemental solids and clusters, surface energy is roughly proportional to (E_c/R^2), where E_c is the cohesive energy and R is the bulk interatomic distance. So, we can get a *rough* estimate of what the slope would be for pure Rb clusters by taking $3.48 \times (0.85/2.95) \times (2.89/4.837)^2$, which is 0.36. So, the slope of 1.26 for the mixed Ag–Rb clusters must surely be very different from the pure Rb_n case also. Looking at N_i for $n = 5$ to 10, we see that it is roughly $n/4$ on average, i.e., a quarter of Ag atoms are "interior atoms" in that size interval. The weighted average $(3/4 \cdot 3.48 + 0.36)/1.75 = 1.70$ is reasonably close to 1.26, so the slope of the fit line in Fig. 3*b*

Fig. 3. Relative isomer energies, and cohesive energies of the GMs.

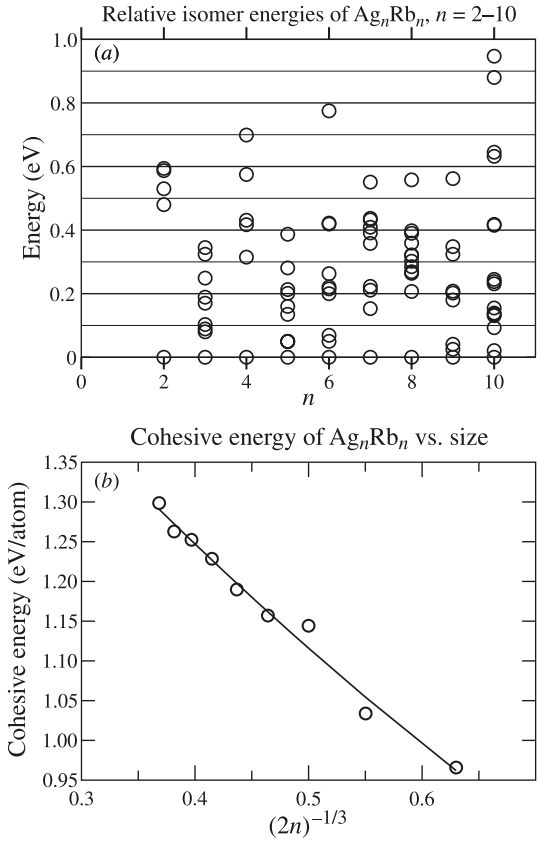

Fig. 4. Global minima.

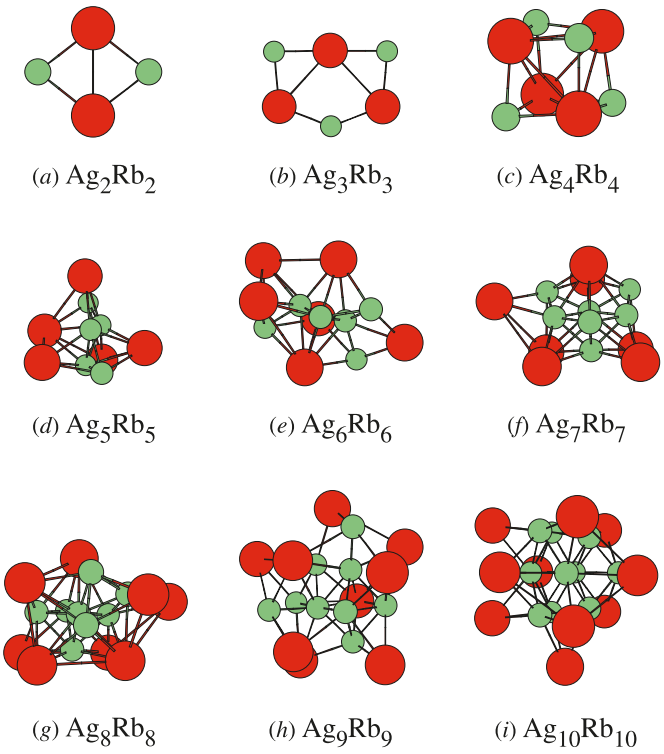

can be understood as a sort of weighted average of the surface energies of Ag and Rb. At very large n, the surface should consist entirely of Rb atoms, and the slope of a straight line fit would have to be close to –0.36, not –1.26. So, clearly, a linear function of $N^{-1/3}$ cannot fit accurately the cohesive energies of Ag_nRb_n over the entire range of n.

The n = 2–4 GM structures are very well-mixed (Figs. 4*a*–4*c*). A natural bond orbital (NBO) analysis reveals atomic charges of nearly ±0.75 in all three cases and shows that bonding is predominantly ionic. The structures in bigger clusters show a strong tendency for Ag atoms to be near the center, and by n = 8, the silver core is already fairly compact and tridimensional. The NBO analysis for $n > 4$ shows that charges are smaller (~ ± 0.50) and that a larger fraction of the valence electrons are delocalized, both of which indicate a transition from ionic to metallic bonding at around n = 5.

We also calculated atomic charges using the self-consistent charge equalization (SC QEq) method,[6,19] which is an improved version of QEq,[20] to gain more insight. In SC QEq, an electronegativity parameter χ is assigned to each element (Ag, Rb), along with parameters for the first, second, and third derivatives of χ with respect to atomic charge. These derivatives also depend on an atom's position, through its screened Coulomb interactions to other atoms, so, for instance, the Ag atoms in a given cluster do not necessarily all end up with the same charge. Atomic charges, and charge-dependent atomic electronegativities, are calculated iteratively until they satisfy the principle of electronegativity equalization.[21,22] An approximate electrostatic energy is then calculated by summing pairwise-screened Coulomb interactions. Details of the method can be found in the literature.[19] For the GM of Ag_nRb_n (n = 2, 3, and 4), the average SC QEq charges on Rb atoms are 0.76, 0.91, and 1.12, respectively. For the GM at n = 5–9, the average SC QEq charges on Rb atoms vary between 0.40 and 0.53 and have no simple relation to n, and for n = 10, it is 0.27. These SC QEq charges are not very different from the NBO charges. The SC QEq electrostatic energy per atom is strongly correlated to the average magnitude of SC QEq charges. So, the different geometric AB ordering of the GMs as a function of n, along with a simple electrostatic model that ignores quantum mechanical effects (SC QEq), are sufficient to explain some qualitative differences in bonding seen in a more rigorous (NBO) analysis. Other interesting things emerge from the SC QEq analysis. First, at $n > 4$, the average magnitudes of SC QEq charges in the GM are neither small or big compared to those in other structures found in our TSDS search. But for $n \leq 4$, the average magnitudes of SC QEq charges in the GMs are much bigger than in the other structures, which indicates ionic bonding in the GMs, and they increase as a function of size (from n = 2 to n = 4), whereas other structures show no clear trend with size. Second, the SC QEq electrostatic energies of the different isomers for a given cluster size vary over a big range: 1.1 eV (n = 2), 2.1 eV (n = 3), 3.5 eV (n = 4), 1.8 eV (n = 5), and for $n > 5$, a typical range is n/2 eV. At $n > 4$, the GMs have SC QEq electrostatic energies that are typically 2–3 eV less negative (less stable) than for the structure with most negative SC QEq electrostatic energy for that size. Third, there is a big drop in the SC QEq average Rb charge between n = 9 (0.47) and n = 10 (0.27) and, linked to that, a big drop in the mixing parameter M (Fig. 5*c*). One could say that Ag_nRb_n clusters ($n \leq 10$) are an example of a frustrated sys-

Fig. 5. Size evolution of structure and properties in the GM of Ag_nRb_n.

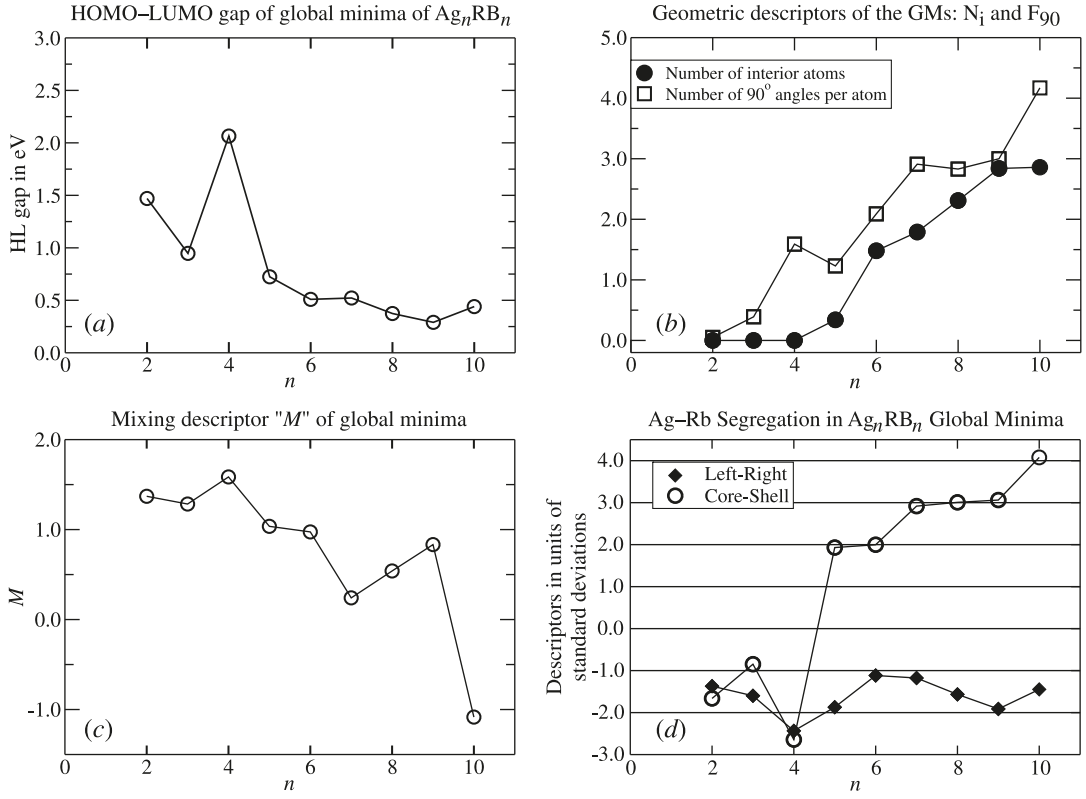

tem. Their lowest-energy structures do not necessarily minimize electrostatic energy, or surface energy (i.e., do not maximize the number of nearest neighbours). Instead, the GM structures are normally the best compromise between these two things, and evolve with size from mixed ($n \leq 4$) to "mostly core-shell segregated" ($n = 10$). We wanted to see how much difference there is between the GM of Ag_nRb_n ($n > 4$) and ideal CSS structures. To do that, we calculated the mean coordination "x" in hypothetical Ag_n clusters that consist of the n Ag atoms at their positions in the GM of Ag_nRb_n, $x(Ag;Ag_nRb_n)$; and for comparison, we calculated the mean coordinations of Ag atoms in the GM of Ag_n clusters that we had previously obtained,[7] $x(Ag;Ag_n)$. In either case, x is the mean number of Ag atom neighbours around a Ag atom. An ideal Ag_nRb_n CSS structure would have a central compact Ag_n subunit with a structure comparable to, and roughly as compact as, that of a pure Ag_n cluster. What we find, going in order from $n = 2$ to $n = 10$, is $x(Ag;Ag_nRb_n)$ = 0.0, 0.0, 0.0, 2.4, 2.3, 3.4, 3.5, 3.3, and 4.6. These values are much smaller than the corresponding $x(Ag;Ag_n)$; going again in order from $n = 2$ to $n = 10$, we have $x(Ag;Ag_n)$ = 1.0, 2.0, 2.5, 2.8, 3.0, 4.6, 4.5, 4.7, and 5.2. We see that the Ag_n subunits in Ag_nRb_n are a lot less compact than Ag_n clusters, except maybe for $n = 5$ and $n = 10$. This again shows that the GM of Ag_nRb_n ($n > 4$) represent a compromise between minimizing surface energy and maximizing ionic energy (mixing).

The size evolution of the HOMO–LUMO gap and some geometric descriptors of the GMs are shown in Fig. 5. The peak in HOMO–LUMO gap at $n = 4$ is remarkable. Two other things indicate special stability for Ag_4Rb_4: the $E(n = 4)$ point is well above the fit line of cohesive energies (Fig. 3*b*), and the second most stable isomer found for Ag_4Rb_4 is much higher (0.3 eV) than the GM (Fig. 3*a*). It is tempting to ascribe that to the eight-electron count, which is a closed shell in the jellium model. However, the difference in bulk electron densities of Ag and Rb, 0.0087 – 0.0017 = 0.0070 au, is very close to the critical value (0.0080 au) beyond which one normally sees inversion of the 2s and 1d jellium levels and magic numbers of 2, 10 (instead of 8), and 20.[3, 23] Also, the large atomic charges (NBO and SC QEq) in Ag_4Rb_4 indicate that ionic bonding is more important than delocalized metallic bonding. The SC QEq electrostatic energy, which is admittedly very approximate, amounts to 60% of the KS-DFT-PBE atomization energy of Ag_4Rb_4. Aside from the anomaly at $n = 4$, and maybe $n = 10$, HOMO–LUMO gaps decrease smoothly from $n = 2$ to $n = 10$, suggesting a gradual transition from ionic to metallic bonding.

There is a rationale for why the transition from mixed to CSS structure should occur near $n = 5$. Ionic bonding favors mixed structures at any size. On the other hand, the difference in surface energies between Ag and Rb, which is *roughly* $E_s(Ag) - E_s(Rb) \approx 0.4 \times (2.95 - 0.85) = 2.1$ eV per surface atom, favors CSS structures, i.e., it disfavors mixing, but only provided that the number of interior atoms (N_i) is not zero of course. Generally speaking, for metal clusters, one expects that N_i becomes nonzero for clusters with more than roughly 12 atoms because the 13-atom icosahedron is the smallest cluster in the polytetrahedral growth sequence with one interior atom. For structures other than polytetrahedral, N_i can become nonzero at slightly smaller or slightly bigger size. In mixed A_nB_n clusters where the el-

ement with lowest cohesive energy has a bigger atomic radius, like Ag_nRb_n, the smallest cluster size with one interior atom can occur at a smaller size, 10 atoms ($n = 5$) in our case (see Fig. 5*b*). As soon as clusters are big enough to accommodate one interior atom, the maximally mixed structure is no longer automatically favored, and the GM are generally "structures of compromise". Using a crude model (see Appendix 1), we estimate that the surface energy of a CSS structure is lower than that of a mixed (ionic) structure by an amount ΔU_s that is roughly $(2n - 8) \times 0.43$ eV in Ag_nRb_n clusters ($n > 4$). On the other hand, as we said earlier, the range in calculated SC QEq electrostatic energies among different isomers of Ag_nRb_n is roughly $0.5n$ eV. So, these two contributions to energy differences between mixed and segregated structures have comparable magnitudes, and they both scale roughly as n, which gives a rationale for why, starting with $n = 5$, the structures of GM are neither of the mixed nor the ideal (compact) core-shell type.

There remains a strong ionic character (charges of ±0.5) even in the largest clusters. This has an effect on the preferred geometries of Ag_nRb_n clusters. In particular, the number of 90° bond angles (F_{90}) per atom is large compared with other metal clusters: F_{90} varies between 1 and 4 for Ag_nRb_n ($n > 3$), and it is 2.1 for $n = 6$ (12-atom cluster) and 2.9 for $n = 7$ (14-atom cluster). The average of 2.1 and 2.9, 2.5, can be compared to the F_{90} value we found for the calculated GM of 26 different 13-atom metal clusters.[17] Of those 26 cases, only six (Tc_{13}, Ru_{13}, Rh_{13}, Re_{13}, Os_{13}, Ir_{13}) had $F_{90} > 2.5$. The large F_{90} values in those six cases were explained by the participation of d orbitals in bonding; but this explanation obviously cannot apply to Ag_nRb_n. The largest F_{90} we calculated[17] for 13-atom clusters of group 1, 2, 11, or 12 in the periodic table was 1.5 (for Zn_{13}), much smaller than 2.5. We think that the large F_{90} in Ag_nRb_n is a consequence of the large ionic contribution to bonding and the effect this has on A–B ordering, since cubic packing (as in NaCl) would minimize the electrostatic energy. The tendency to adopt structures with large F_{90} is not limited to the GM of Ag_nRb_n; several isomers (some of them not shown here) have prismatic or square arrangements of Rb atoms, e.g., Fig. 2*g* and 2*k*. It is also interesting to track the number of interior atoms, N_i, as a function of n (see Fig. 5*b*), but we are unable to predict accurately the size where $N_i = n$, i.e., the smallest cluster with n interior Ag atoms covered by a "monolayer" of n Rb atoms (this would correspond to the closure of an atomic shell in the core-shell growth sequence and could give enhanced stability). A simple geometric model leads us to predict that, within the Ag_nRb_n sequence, the Rb shell of the atoms becomes complete only at $n = 30$, *roughly*.

The mixing descriptor M and core-shell segregation parameter C (Figs. 4*j* and 4*k*) both undergo a sudden change between $n = 4$ and $n = 5$. The value of M starts off very large (at $n = 2$) and goes down but remains above zero until $n = 10$. As expected, the large electronegativity difference between Ag and Rb favors mixing. The drop of M at $n = 10$ shows that the driving force for having Ag atoms inside (difference in surface energies of Ag and Rb) is bigger than the driving force for mixing (difference in electronegativities of Ag and Rb). There is no special significance to M becoming negative at precisely $n = 10$. It happens partly because, with increasing number of atoms, there are many more ways to make highly mixed homotops, which makes the CSS structures appear poorly mixed in a relative sense (see eq. [4]). The C values get very large at $n > 4$ (+2.0 to +4.0) while L always stays negative; this shows that Ag_nRb_n has indeed a strong tendency to form core-shell structures, even for n values as small as 5.

The shape descriptor, $\eta = (2I_b - I_a - I_c)/I_a$, of the GMs of Ag_nRb_n is negative for $2n = 4$, 6, 14, 16, and 18, positive for $2n = 10$ and 12, and very nearly zero for $2n = 8$ and 20. These predictions of oblate, prolate, and spherical shapes agree with the ellipsoidal jellium model in every case except Ag_2Rb_2. The peaks in the HOMO–LUMO gap at $2n = 8$ and 20 also agree with the jellium model, but this is partly coincidental. For instance, the structure of Ag_4Rb_4 is optimal for ionic bonding (it is cubic), and also for accomodating a spherical closed-shell of eight electrons ($I_a = I_b = I_c$) as per the jellium model, but bonding in Ag_4Rb_4 is predominantly ionic. However, the agreement of DFT and EJM cluster shapes for all cases at $n \geq 5$ is probably not entirely accidental either. The EJM may be a crude model of electronic structure, but it gives a qualitatively correct relation between cluster shape and orbital symmetry and energies. These effects of shape and orbital symmetry are implicitly included in a more complete theory like DFT and may well give a small energetic preference (maybe in the order of a few tenths of eV) to structures that conform to the EJM.

In conclusion, the structures and nature of chemical bonding in Ag_nRb_n clusters evolve from mixed AB structures having ionic bonding for $n \leq 4$ to CSS structures where metallic bonding dominates but where ionic bonding is still important for $n = 5$ to 10. The Ag_4Rb_4 clusters are special for their relative stabilities and large HOMO–LUMO gaps. The geometric structures of Ag_nRb_n ($n = 5$ to 10) have a Ag core and an incomplete Rb shell, but the Ag core is not very compact. These structures are the result of a compromise between metallic and ionic contributions to bonding. Atomic charges on the Rb outer-shell atoms in $Ag_{10}Rb_{10}$ are calculated to be +0.3; this may be large enough to prevent coalescence of larger $Ag_n@Rb_n$ clusters having a complete Rb outer shell.

Acknowledgements

RF is grateful to the European Science Foundation (ESF) for supporting the *2008 Workshop on Computational Nanoalloys* where participants discussed many ideas that are relevant to the work presented here, and to the Natural Sciences and Engineering Research Council of Canada (NSERC) for research funding.

References

(1) This article is part of a Special Issue dedicated to Professor T. Ziegler.
(2) This manuscript is dedicated to Tom Ziegler on the occasion of his 65th birthday.
(3) Alonso, J. A; *Structure and properties of atomic nanoclusters*; Imperial College Press: London, 2005.
(4) Ferrando, R.; Jellinek, J.; Johnston, R. L. *Chem. Rev.* **2008**, *108* (3), 845–910. doi:10.1021/cr040090g.
(5) Paz-Borbón, L. O.; Gupta, A.; Johnston, R. L. *J. Mater. Chem.* **2008**, *18* (35), 4154. doi:10.1039/b805147j.

(6) Zhang, M.; Fournier, R. *J. Mol. Struct. THEOCHEM* **2006**, *762* (1-3), 49–56. doi:10.1016/j.theochem.2005.08.042.
(7) Fournier, R. *J. Chem. Phys.* **2001**, *115* (5), 2165. doi:10.1063/1.1383288.
(8) Bhaskar, N. D.; Frueholz, R. P.; Klimcak, C. M.; Cook, R. A. *Phys. Rev. B* **1987**, *36* (8), 4418–4421. doi:10.1103/PhysRevB.36.4418.
(9) (a) de Heer, W. A. *Rev. Mod. Phys.* **1993**, *65* (3), 611–676. doi:10.1103/RevModPhys.65.611.; (b) Brack, M. *Rev. Mod. Phys.* **1993**, *65* (3), 677–732; and refs. therein. doi:10.1103/RevModPhys.65.677.
(10) Corbett, J. D. *Angew. Chem., Int. Ed.* **2000**, *39* (4), 670–690. doi:10.1002/(SICI)1521-3773(20000218)39:4<670::AID-ANIE670>3.0.CO;2-M.
(11) Cheng, J.; Fournier, R. *Theor. Chem. Acc.* **2004**, *112*, 7.
(12) (a) Perdew, J. P.; Burke, K.; Ernzerhof, M. *Phys. Rev. Lett.* **1996**, *77* (18), 3865–3868. doi:10.1103/PhysRevLett.77.3865. PMID:10062328.; (b) Perdew, J. P.; Burke, K.; Ernzerhof, M. *Phys. Rev. Lett.* **1997**, *78* (7), 1396. doi:10.1103/PhysRevLett.78.1396.
(13) Frisch, M. J.; Trucks, G. W.; Schlegel, H. B.; Scuseria, G. E.; Robb, M. A.; Cheeseman, J. R.; Montgomery, J. A., Jr.; Vreven, T.; Kudin, K. N.; Burant, J. C.; Millam, J. M.; Iyengar, S. S.; Tomasi, J.; Barone, V.; Mennucci, B.; Cossi, M.; Scalmani, G.; Rega, N.; Petersson, G. A.; Nakatsuji, H.; Hada, M.; Ehara, M.; Toyota, K.; Fukuda, R.; Hasegawa, J.; Ishida, M.; Nakajima, T.; Honda, Y.; Kitao, O.; Nakai, H.; Klene, M.; Li, X.; Knox, J. E.; Hratchian, H. P.; Cross, J. B.; Bakken, V.; Adamo, C.; Jaramillo, J.; Gomperts, R.; Stratmann, R. E.; Yazyev, O.; Austin, A. J.; Cammi, R.; Pomelli, C.; Ochterski, J. W.; Ayala, P. Y.; Morokuma, K.; Voth, G. A.; Salvador, P.; Dannenberg, J. J.; Zakrzewski, V. G.; Dapprich, S.; Daniels, A. D.; Strain, M. C.; Farkas, O.; Malick, D. K.; Rabuck, A. D.; Raghavachari, K.; Foresman, J. B.; Ortiz, J. V.; Cui, Q.; Baboul, A. G.; Clifford, S.; Cioslowski, J.; Stefanov, B. B.; Liu, G.; Liashenko, A.; Piskorz, P.; Komaromi, I.; Martin, R. L.; Fox, D. J.; Keith, T.; Al-Laham, M. A.; Peng, C. Y.; Nanayakkara, A.; Challacombe, M.; Gill, P. M. W.; Johnson, B.; Chen, W.; Wong, M. W.; Gonzalez, C.; Pople, J. A. *Gaussian 03*, Revision C.02; Gaussian, Inc.: Wallingford, CT, 2004.
(14) (a) Chekmarev, S. F. *Phys. Rev. E Stat. Nonlin. Soft Matter Phys.* **2001**, *64* (3 Pt 2),o. 036703. PMID:11580478.; (b) Tsai, C. J.; Jordan, K. D. *J. Phys. Chem.* **1993**, *97* (43), 11227–11237. doi:10.1021/j100145a019.
(15) Jellinek, J.; Krissinel, E. B. *Chem. Phys. Lett.* **1996**, *258* (1-2), 283–292. doi:10.1016/0009-2614(96)00636-7.
(16) Fournier, R. *J. Chem. Theory Comput.* **2007**, *3* (3), 921–929. doi:10.1021/ct6003752.
(17) Sun, Y.; Zhang, M.; Fournier, R. *Phys. Rev. B* **2008**, *77* (7),o. 075435. doi:10.1103/PhysRevB.77.075435.
(18) (a) Wales, D.; Doye, J. *J. Phys. Chem. A* **1997**, *101* (28), 5111–5116. doi:10.1021/jp970984n.; (b) Doye, J.; Wales, D. *Phys. Rev. Lett.* **1998**, *80* (7), 1357–1360. doi:10.1103/PhysRevLett.80.1357.
(19) Zhang, M.; Fournier, R. *J. Phys. Chem. A* **2009**, *113* (13), 3162–3170. doi:10.1021/jp8063273. PMID:19320517.
(20) Rappe, A. K.; Goddard, W. A., III. *J. Phys. Chem.* **1991**, *95* (8), 3358–3363. doi:10.1021/j100161a070.
(21) Sanderson, R. T. *Science* **1951**, *114* (2973), 670–672. doi:10.1126/science.114.2973.670. PMID:17770191.
(22) Sanderson, R. T; *Chemical bonds and bond energy*; 2nd ed; Academic Press: New York, 1976.
(23) Baladrón, C.; Alonso, J. A. *Physica B* **1988**, *154* (1), 73–81. doi:10.1016/0921-4526(88)90019-1.
(24) Somorjai, G. A; *Introduction to surface chemistry and catalysis*; Wiley: New York, 1994.

Appendix I. Model of surface energy in mixed and core-shell A_nB_n clusters

We want to estimate the energy difference, ΔU_s, arising from the different surface area, structure, and composition at the surface of two qualitatively different types of A_nB_n cluster structures (ionic and maximally mixed (IMM), and core-shell (CS)). A model like SC QEq could be used to estimate energy differences due to electrostatics, ΔU_e. The sign of $\Delta U_s + \Delta U_e$ could then be used to make qualitative predictions of cluster structure in A_nB_n mixed clusters.

We assume that IMM clusters have a packing similar to the simple cubic crystal structure and have a cubic shape, whereas the CS clusters are spherical with atoms packed in a way similar to fcc. These assumptions clearly cannot be exact for small clusters, but they hopefully capture an essential difference in the surface-to-volume ratio for the two types. So, the volume V and surface area A of the two structure types are estimated to be

$$[A1] \qquad \begin{matrix} \text{IMM} \left\{ \begin{matrix} V = Nv\sqrt{2} \\ A = 6V^{2/3} = 7.560(Nv)^{2/3} \end{matrix} \right\} \\ \text{CS} \quad \left\{ \begin{matrix} V = Nv \\ A = 4.836V^{2/3} = 4.836(Nv)^{2/3} \end{matrix} \right\} \end{matrix}$$

where $N = 2n$ is the number of atoms and v is the average of the bulk atomic volumes for elements A and B. The surface of an IMM cluster is assumed to have A–B composition of 50%:50%, so the surface energy for IMM can be estimated as

$$[A2] \qquad U_s = (A_{IMM}/a)E_c \times 0.4$$

where E_c is the average of the two cohesive energies ((0.85 + 2.95)/2 = 1.90 eV for Ag–Rb) and a is the square of the average of bulk A–A and B–B distances (14.9 Å^2 for Ag–Rb); a is a rough estimate of surface area per atom in a mixed ordered A–B surface. The factor 0.4 is empirical; a factor of 0.16 would be appropriate for surface atoms of macroscopic particles,[24] but the cohesive energy of very small metal clusters (those with $N_i = 0$) is often close to 60% of the bulk cohesive energy, which motivates the choice of 0.4. The composition of the surface of a CS cluster depends on the number N_i of interior atoms. If N_i is large enough, the surface of CS clusters have only atoms of type "B" (the one with lowest surface energy), and in this particular case, the surface energy of the CS cluster would be

$$[A3] \qquad U_s = (A_{CS}/R_B^2)E_{c,B} \times 0.4$$

Let us define $f_m = 7.56E_c/a$ and $f_c = 4.836E_{c,B}/R_B^2$. Then, the surface energy for IMM is $f_m \times 0.4 \times (Nv)^{2/3}$, and the surface energy of a very large CS cluster is $f_c \times 0.4 \times (Nv)^{2/3}$. For the Ag–Rb case, $0.4 \times v^{2/3} = 4.78$ Å^2. When a CS cluster is not too large, there are $N_i < n$ interior atoms, and the surface composition is not 100% B. Instead, it is closer to $(N/2 - N_i)$ atoms of A and $N/2$ atoms of B, or alter-

natively, $(N - 2N_i)$ of AB, and N_i of B. So, we calculate a factor f_x for intermediate size CS cluster like this:

$$[A4] \qquad f_x = [(N - 2N_i)f_m + N_i f_c]/(N - N_i)$$

and estimate the surface energy of the CS cluster as

$$[A5] \qquad \begin{aligned} U_s &= f_x \times 0.4 \times (Nv)^{2/3} \\ &= f_x \times 4.78 \times N^{2/3} \text{ for Ag}-\text{Rb} \end{aligned}$$

From our calculated N_i values (Fig. 5*b*), we can propose a simplified approximate relation between N_i and N, $N_i \approx (N - 4)/2$. Using this relation and the equations above, we can estimate the contribution ΔU_s to the energy difference between IMM- and CS-type structures that is specifically due to surface structure and composition. We find $\Delta U_s = 0$, 1.8, 3.4, and 4.9 eV for $N = 8$, 12, 16, and 20, respectively.